Chemical Engineering Journal 172 (2011) 713–720

Contents lists available at ScienceDirect

Chemical Engineering Journal

journal homepage: www.elsevier.com/locate/cej

A resin with high adsorption selectivity for Au (III): Preparation, characterization and adsorption properties

Sun Changmei, Zhang Guanghua, Wang Chunhua, Qu Rongjun*, Zhang Ying, Gu Quanyun

School of Chemistry and Materials Science, Ludong University, Yantai 264025, China

ARTICLE INFO

Article history:
Received 27 April 2011
Received in revised form 16 June 2011
Accepted 17 June 2011

Keywords:
Polystyrene-supported
3-amino-1,2-propanediol
Preparation
Adsorption
Selectivity
Au(III)

ABSTRACT

In this paper, a novel chelating resin with high adsorption selectivity for Au (III), polystyrene-supported 3-amino-1,2-propanediol (PS-APD), was prepared simply by the reaction of chloromethylated polystyrene with 3-amino-1,2-propanediol. Its structure was characterized by infrared spectroscopy (IR), scanning electron microscope (SEM) and porous structure analysis. The adsorption capabilities of PS-APD for Pb(II), Hg(II), Cu(II), Ni(II) and Au(III) ions were investigated. The results suggested that PS-APD resin possessed much better adsorption capability for Au(III) than for other metal ions. A comparison of the kinetic models on the overall adsorption rate showed that adsorption system was best described by the pseudo second-order kinetics. The adsorption equilibrium data fitted best with the Langmuir isotherm and thermodynamic parameters including ΔG, ΔH and ΔS were calculated. The adsorption mechanism of PS-APD for Au(III) was confirmed by SEM, IR and X-ray photoelectron spectroscopy (XPS), which showed that redox reaction occurred between 3-amino-1,2-propanediol group and Au(III) ions. Adsorption selectivity experiments indicated that PS-APD resin possessed excellent adsorption property to Au(III) ions, offering potential applications in recovery of Au(III) from multi-ionic aqueous systems.

1. Introduction

Because of its specific physical and chemical properties, gold is widely used in many fields such as catalysts in various chemical processes, electrical and electronic industries, corrosion resistant materials and jewellery [1,2]. Economically, gold has been historically important as currency, and remain important as investment commodity. Considering its value and scarcity, it is necessary to treat the waste aqueous solutions and try to recover gold economically. Nevertheless, the separate and recovery of gold is not actually simple, which is due to the low concentration of gold in environmental, geological and metallurgical materials and insufficient sensitivity. At present, many methods such as co-precipitation [3], ion exchange [4,5] and solvent extraction [6] and adsorption [7,8] have been used to separate and enrich gold. Comparatively, the adsorption of a solute on a solid support has the advantage over liquid–liquid extraction in that no mixing and settling requirements have to be fulfilled and organic phase loss through entrainment is eliminated. And the chelating adsorption seems to be the most suitable method for the recovery of precious metals in the case of low concentration due to low cost and high efficiency [9].

Resins functionalized with groups containing nitrogen or sulfur can be efficient in the adsorption of metal ions [10–15]. Recently, we functionalized polystyrene resin with 3-amino-1,2-propanediol (APD) group, which is an important medical intermediate with very low toxicity. Originally, we designed this resin in order to selective adsorption for copper ions because the structure of APD was similar to that of glycerol, which can form stable complex compound with copper ions. However, with the proceeding of adsorption experiments, we found that the resin exhibited much better selective adsorption capability for gold ions than for copper ions, which was different from what we expected before. Therefore, the adsorption properties of polystyrene supported 3-amino-1,2-propanediol (PS-APD) resin for Au(III) including adsorption selectivity, adsorption kinetics and adsorption isotherm were investigated in detail in this paper.

2. Experimental

2.1. Materials and instruments

Polystyrene was obtained from Wandong Chemical Reagent Co., Ltd., China. Chloromethylated polystyrene (PS-Cl) was prepared according to the method described in Ref [16]. 3-Amino-1,2-propanediol (APD) was obtained from Laiyang chemical factory, China. Au(III) solution was prepared using $HAuCl_4{\cdot}4H_2O$ (Fuchen Chemical Reagent Co., Ltd., China) dissolved in distilled water. The

* Corresponding author. Tel.: +86 535 6699201.
E-mail addresses: rongjunqu@sohu.com, qurongjun@eyou.com (Q. Rongjun).

1385-8947/$ – see front matter © 2011 Elsevier B.V. All rights reserved.
doi:10.1016/j.cej.2011.06.040

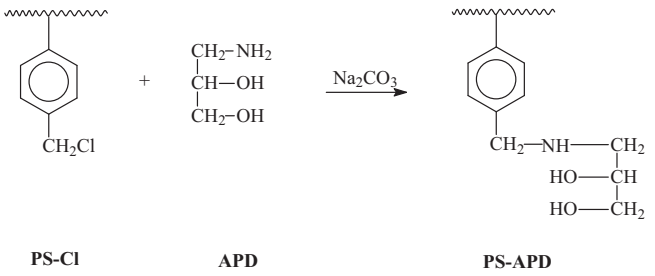

Scheme 1. The synthesis route of PS-APD.

pH values of the solution were controlled with a Seven Multi pH meter, Mettler Toledo Instruments (Shanghai) Co. Ltd., China. All other reagents were of analytical grade and used without further purification.

Infrared spectra (IR) were recorded on a Nicolet MAGNA-IR 550 (Series II) spectrophotometer with testing conditions: potassium bromide pellets, scanning 32 times, resolution 4 cm^{-1}. Porous structure parameters were characterized using an automatic physisorption analyzer (ASAP 2020, Micromeritics, USA) using BET and BJH methods through N_2 adsorption at 77 K. The shape and surface morphology of the resins were examined on a scanning electron microscope (SEM), JSF5600LV, JEOL, Japan. Atomic absorption analysis of the various metal ions was performed with a flame atomic absorption spectrophotometer (Model 932B, GBC Scientific Equipments Pvt. Ltd., Australia). X-ray photoelectron spectroscopy (XPS) spectra were collected on PHI 1600ESCA system, Perkin-Elmer Co., USA, with testing conditions: MgKa (1253.6 eV), power 200.0 W, resolution 187.85 Ev.

2.2. Preparation of polystyrene supported 3-amino-1,2-propanediol (PS-APD)

The preparation procedure is simple and described as follows. A mixture of chloromethylated polystyrene (PS-Cl, 5.0 g) and dimethylformamide (100 mL) was refluxed for 2 h with continuous stirring, then APD (10 mL) and Na_2CO_3 (2.0 g) was added. The mixture was refluxed for 8 h at 80 °C with stirring under nitrogen atmosphere. The solid product was then filtered off and transferred to the Soxhlet extraction apparatus for reflux-extraction in ethanol for 10 h. After extraction, the product was dried under vacuum at 50 °C over 48 h and resin PS-APD was obtained. The synthesis route of PS-APD was presented in Scheme 1.

The mass percentage of nitrogen on the surface of PS-APD measured by X-ray photoelectron spectroscopy was 2.9%. Divide mole mass of N atom 14 by 2.9%, the content of N-containing groups on the surface of the resin beads was obtained as 2.07 mmol g^{-1}.

2.3. Comparative study

Static adsorption experiment was employed to determine the adsorption capabilities of adsorbent for different metal ions. The 0.1 mol L^{-1} stock solutions of Cu(II) and Ni(II) were prepared in distilled water and the those 0.1 mol L^{-1} Pb(II) and Hg(II) were prepared in 2% HNO_3. Buffer solution of acetic acid/acetate (pH 4.0) was used for the experiments.

Static adsorption experiments were carried out by shaking 40 mg of PS-APD with 20 mL of solution containing metal ions with concentration of 5×10^{-3} mol L^{-1}. The mixture was equilibrated for 24 h on a thermostat-cum-shaking assembly at 25 °C. Then a certain volume of the solutions was separated from the adsorbent and the residual concentration of metal ions was detected by means of AAS. The adsorption amounts were calculated according to the following Eq. (1)

$$Q = \frac{(C_0 - C)V}{W} \quad (1)$$

The adsorption percentages of PS-APD for metal ions were calculated to the following Eq. (2):

$$\text{Adsorption percentage}(\%) = \frac{C_0 - C}{C_0} \times 100 \quad (2)$$

where Q is the adsorption amount (mmol g^{-1}), C_0 and C, the initial and the final concentrations of metal ions in solution, respectively (mmol L^{-1}); V, the volume (L); W, the weight of PS-APD (g).

2.4. Kinetic adsorption

Batch tests were performed to determine kinetic adsorption properties of PS-APD for Au(III) ions. A typical procedure is: 0.01 g of PS-APD was shaken with 10 mL of solution containing Au(III) ions for different hours. After the centrifugation, 4 mL solution was taken out and put in 25 mL colorimetry-used tube, and the distilled water was put in until the whole volume was 25 mL, and the concentration of Au(III) was determined by AAS. The adsorption amount was calculated according to Eq (1).

2.5. Adsorption isotherm

The isothermal adsorption was investigated by batch tests. A typical procedure is as follows: a series of 100 mL iodine flasks with ground-in glass stopper were employed. Each flask was filled with 10 mL of Au(III) solution of varying concentrations. A known amount of adsorbents (about 30 mg) was added into each flask and agitated intermittently at 25 °C for 24 h. The adsorption capacities were calculated using Eq. (1), where C is the equilibrium concentration of Au(III) in solution.

2.6. Adsorption selectivity

40 mg of PS-APD was placed in a 100 mL iodine flask, then 2 mL of Au (III) with concentration 2.43×10^{-2} mol L^{-1}, 1 mL of coexistent metal ion with concentration 0.1 mol L^{-1} and 17 mL of buffer solution (pH 4.0) were added in turn. The mixture was shaken for 24 h at 25 °C. After the centrifugation, the concentrations of Au(III) and the coexistent metal ion were determined by AAS. The adsorption capacities of Au(III) and the coexistent metal ion were calculated according to Eq. (1). The adsorption selectivity was determined by Eq. (3).

$$\text{Sel}_i = \log \frac{(Q_e/C_e)_i}{(Q_e/C_e)_j} \quad (3)$$

where Q_e is the amount of metal adsorbed at equilibrium per unit weight of adsorbent (mmol g^{-1}); C_e is the equilibrium concentration of metal ions in solution (mmol L^{-1}). The index i pertains to gold in this paper and index j refers to the remaining metals in the solution other than i.

3. Results and discussion

3.1. IR spectroscopy analysis

IR is usually employed to monitor the immobilization process by comparing the precursor and product. The infrared spectra of the original and chemically modified chloromethylated polystyrene were presented in Fig. 1. It could be seen that the two characteristic peaks for C–Cl at 1264 and 676 cm^{-1} [17] almost disappeared and

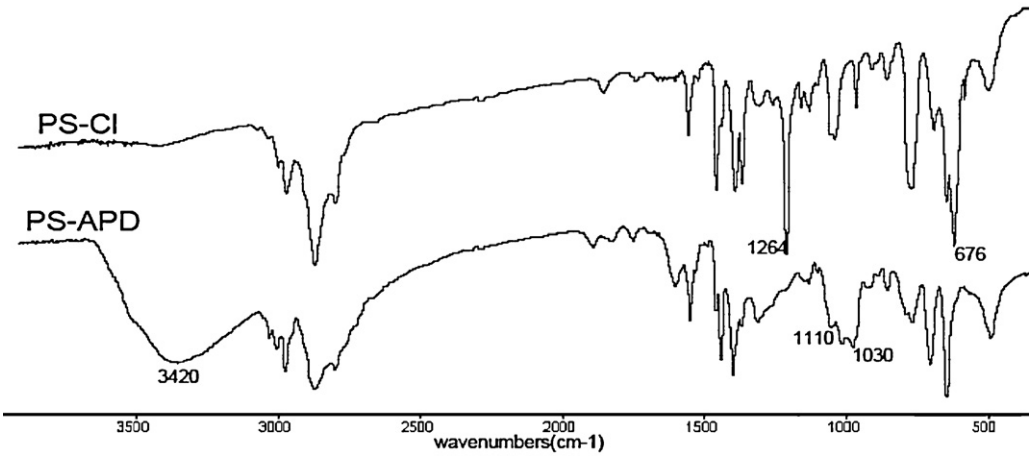

Fig. 1. Infrared spectra of PS-Cl and PS-APD.

Table 1
The porous structure parameters of PS-Cl and PS-APD.

Adsorbents	BET surface area ($m^2\ g^{-1}$)	BJH desorption cumulative volume of pores ($cm^3\ g^{-1}$)	BJH desorption average pore diameter (nm)
PS-Cl	26.670	0.388	41.47
PS-APD	25.171	0.239	35.49

some new peaks appeared between 1030 and 1100 cm^{-1} attributing to the characteristic absorption of C–O after the reaction of PS-Cl with APD. The characteristic absorption of O–H and N–H in PS-APD groups appeared around 3420 cm^{-1} [18], confirming that APD groups were successfully introduced into PS-Cl matrix.

3.2. Pore structure analysis

BJH desorption pore size distributions of PS-Cl and PS-APD were shown in Fig. 2. As illustrated in Fig. 2, the pores between 30 and 70 nm were dominant for both resins. Also it could be seen that the volumes of the pores between 30 and 70 nm for PS-APD were smaller than those for PS-Cl, but it was contrary to the ones below 20 nm. The porous structure parameters of PS-Cl and PS-APD from the basis of the nitrogen adsorption data were summarized in Table 1. As shown in Table 1, the values of BET surface area, BJH desorption average pore diameter and BJH desorption cumulative volume of pores for PS-APD were all smaller than those for PS-Cl. The decrease of the pore size could be attributed to the introduction of organic groups in the pores, which blocked the adsorption of nitrogen molecules [19].

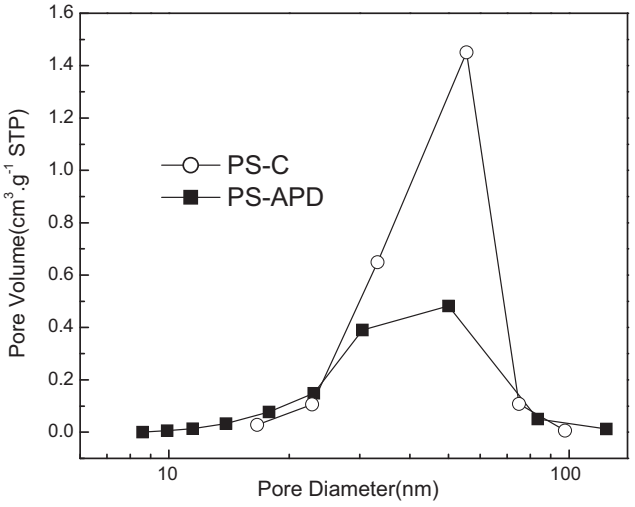

Fig. 2. BJH desorption pore size distributions of PS-Cl and PS-APD.

3.3. Comparative study

As we know, saturated adsorption capacities for metal ions are essential parameters for evaluating the ability of absorbents to bind and extract different metal ions from aqueous solutions. Table 2 showed the saturation adsorption capacities and adsorption percentage of PS-APD resin for Pb(II), Hg(II), Cu(II), Ni(II) and Au(III) ions. Obviously, the PS-APD had better adsorption capacity for Au(III) than for other metal ions. Because of the highest adsorption capacity, Au (III) ion was selected as representative to be studied the adsorption kinetics and isothermal adsorption of PS-APD in the following part.

3.4. Kinetics studies

The adsorption kinetics data of Au(III) on PS-APD was showed in Fig. 3. It could be seen that the adsorptions at different temperatures were quick at the beginning, and then slow. Temperature affected the adsorption significantly, that is, the adsorption speed increased with the increasing temperature. The possible explanations for this were: (1) the PS-APD resin was swollen more completely at higher temperature, which made metal ions diffuse more easily into the inside of resin; (2) the adsorption was an endothermal process and high temperature was of benefit to the adsorption [20].

Adsorption kinetics parameters, which can control the residence time of the adsorbate uptake at the solution–solid interface and provide valuable insights into water treatment process design, are of great importance for the application of adsorbents. Both pseudo first-and second-order models can be used to express the adsorption process of PS-APD for Au(III). According to the previous

Table 2
The saturated adsorption capacity of PS-APD for metal ions.

Metal ions	Adsorption capacity ($mmol\ g^{-1}$)	Adsorption percentage (%)
Pb(II)	0.177	7.5
Hg(II)	0.747	50.0
Cu(II)	0.446	18.9
Ni(II)	0.128	5.7
Au(III)	1.107	99.1

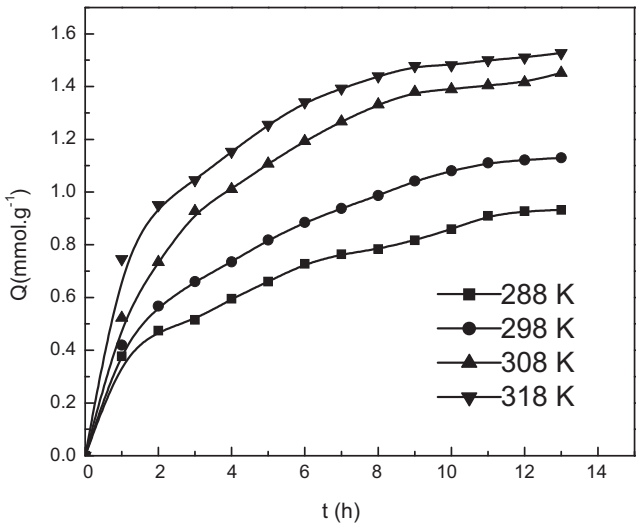

Fig. 3. Adsorption kinetics of PS-APD for Au(III) at different temperatures.

investigations [21,22], the pseudo first- and second-order models can be expressed by Eqs. (4) and (5), respectively.

$$\frac{dQ}{dt} = k_1(Q_e - Q_t) \tag{4}$$

$$\frac{dQ}{dt} = k_2(Q_e - Q_t)^2 \tag{5}$$

Integrating Eqs. (4) and (5) for the boundary conditions $t = 0$ to $t = t$ and $Q_t = 0$ to $Q_t = Q_0$, the equations can be rearranged to obtain the following Eqs. (6) and (7)

$$\ln\frac{(Q_e - Q_t)}{Q_e} = -k_1 t \tag{6}$$

$$\frac{t}{Q_t} = \frac{1}{k_2 Q_e^2} + \frac{t}{Q_e} \tag{7}$$

where Q_e is the amount of metal adsorbed at equilibrium per unit weight of adsorbent (mmol g^{-1}); Q_t is the amount of metal adsorbed at any time (mmol g^{-1}); k_1 and k_2 are the rate constant of pseudo first-order (h^{-1}) and second-order (g $mmol^{-1}$ h^{-1}) adsorption.

The initial adsorption rate is presented by Ho [23]:

$$h = k_2 Q_e^2 \tag{8}$$

where Q_e is the amount of metal adsorbed at equilibrium per unit weight of adsorbent (mmol g^{-1}), k_2 is the rate constant of pseudo second-order (g $mmol^{-1}$ h^{-1}) adsorption.

The plots of $\ln(Q_e - Q_t)$ versus t and t/Q_t versus t were employed to test the pseudo first- and second-order models, respectively. The results were shown in Fig. 4.

As can be seen from Fig. 4, the results obtained for adsorption of Au(III) onto PS-APD were more fitted well to Eq. (7) instead of Eq. (6). The fitting kinetic parameters were listed in Table 3. The results clearly showed that the pseudo second-order model provided better correlation coefficients than pseudo first-order model, suggesting the pseudo second-order model was more suitable to describe the adsorption kinetics processes of PS-APD for Au(III). This revealed that the rate limiting step may be chemical sorption involving valency forces through sharing or exchange of electrons between chitosan and Au(III) [24]. Also we could see that the values of initial adsorption rate h increased with temperature, probably because of the faster diffusion rate of Au(III) under higher temperature.

The intraparticle diffusion model is presented by the following equation [25]:

$$Q_t = k_{int} t^{0.5} + C \tag{9}$$

where k_{int} is the intraparticle diffusion rate constant (mmol g^{-1} $h^{-0.5}$). If intraparticle diffusion is involved in the adsorption process, then the plot of square root of time against the uptake (Q_t) would result in a linear relationship and the intraparticle diffusion would be the controlling step if this line passes through the origin.

For intraparticle diffusion model, even though there was excellent linearity of the plots of square root of time against uptake (Q_t), they did not have zero intercepts (Fig. 5.), indicating that intraparticle diffusion may be involved in the adsorption process but it may not be the controlling factor in determining the kinetics of the process [26].

3.5. Adsorption isotherm

Langmuir and Freundlich isotherms are the most commonly used isotherms for different adsorbent/adsorbate systems to explain solid–liquid adsorption systems and to predict their equilibrium parameters [27]. The Langmuir isotherm is based on the monolayer adsorption on the active sites of the adsorbents. The Langmuir isotherm can be expressed as Eq. (10):

$$Q_e = \frac{Q_m K_L C_e}{1 + K_L C_e} \tag{10}$$

where C_e is the equilibrium concentration of metal ions in solution (mmol L^{-1}); Q_e, the adsorbed value of metal ions at equilibrium concentration (mmol g^{-1}); Q_m, the maximum adsorption capacity (mmol g^{-1}) and K_L is the binding constant which is related to the

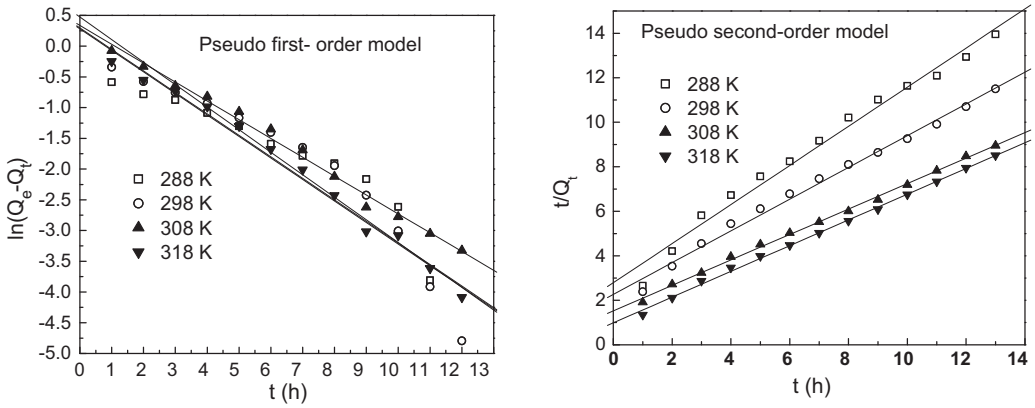

Fig. 4. Pseudo first- and second-order models of PS-APD for Au(III) at different temperatures.

Table 3
Kinetic parameters obtained from pseudo first- and second-order models of PS-APD for Au(III) at different temperatures.

T (K)	$Q_{e,exp}$ (mmol g^{-1})	Pseudo first-order model			Pseudo second-order model			
		k_1 (h^{-1})	$Q_{e.cal,1}$ (mmol g^{-1})	R^2	k_2 (g mmol^{-1} h^{-1})	h (mmol g^{-1} h^{-1})	$Q_{e.cal,2}$ (mmol g^{-1})	R^2
288	0.932	0.350	1.325	0.7954	0.278	0.359	1.137	0.9837
298	1.130	0.367	1.607	0.9057	0.225	0.442	1.402	0.9916
308	1.452	0.307	1.399	0.9911	0.219	0.656	1.729	0.9980
318	1.527	0.350	1.347	0.9877	0.331	1.013	1.748	0.9979

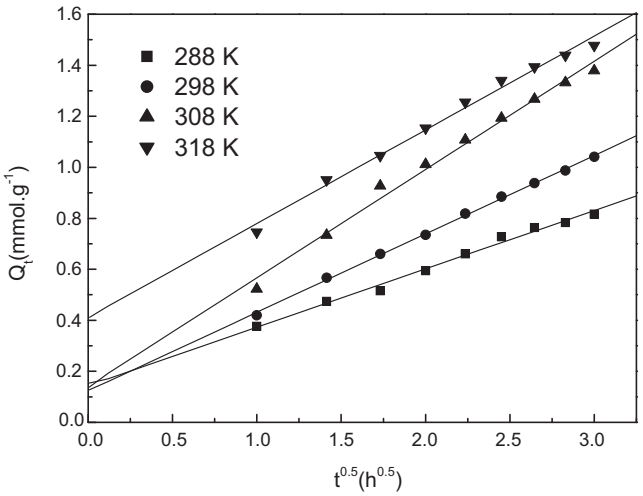

Fig. 5. Plot of intraparticle diffusion model.

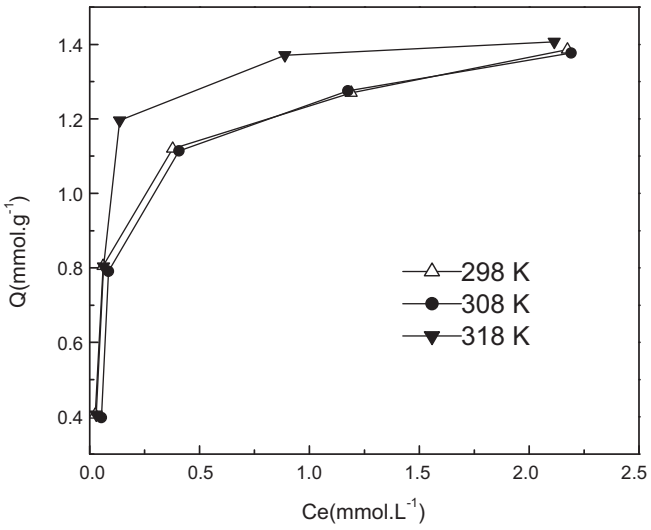

Fig. 6. The isotherms of Au(III) adsorption on PS-APD at different temperatures.

energy of adsorption. For fitting the experimental data, the Langmuir model is linearized as:

$$\frac{C_e}{Q_e} = \frac{C_e}{Q_m} + \frac{1}{K_L Q_m} \tag{11}$$

The Freundlich isotherm explains the adsorption on a heterogeneous (multiple layer) surface with uniform energy. The Freundlich model is represented by Eq. (12):

$$Q_e = K_F C_e^{1/n} \tag{12}$$

where K_F (mmol g^{-1}) is the Freundlich constant related to adsorption capacity of adsorbent and n is the Freundlich exponent related to adsorption intensity (dimensionless). For fitting the experimental data, the Freundlich model is linearized as follows:

$$\ln Q_e = \ln K_F + \frac{1}{n} \ln C_e \tag{13}$$

In this study, the experimental data in Fig. 6 were fitted using Langmuir and Freundlich equations by linear methods and the corresponding adsorption parameters along with correlation coefficients were listed in Table 4.

From Table 4, it could be seen that the correlation coefficient R^2 of linear Langmuir isothermal models are more than 0.99, suggesting that Langmuir isothermal models could be used to describe the isotherm adsorptions of PS-APD resins for Au(III) under the present conditions. The best-fit experimental equilibrium data in Langmuir isotherm suggested the monolayer coverage and chemisorption of Au(III) onto PS-APD. The n values are between 2 and 5, indicating the adsorption processes were carried out easily [28].

Table 5
The parameters of kinetic models of PS-APD for Au (III).

T (K)	ΔG (kJ mol^{-1})	ΔH (kJ mol^{-1})	ΔS (J K^{-1} mol^{-1})
298	−7.14		
308	−8.45	31.90	130.57
318	−9.76		

3.6. Thermodynamic studies

The thermodynamic parameters for the adsorption process such as free energy of adsorption (ΔG), enthalpy of adsorption (ΔH), and entropy of adsorption (ΔS) were calculated by the following Van't Hoff equation (14) [29] and Eq. (15):

$$\ln K_L = \frac{\Delta S}{R} - \frac{\Delta H}{RT} \tag{14}$$

$$\Delta G = \Delta H - T\Delta S \tag{15}$$

where K_L is Langmuir constant; R, gas constant (8.314 J mol^{-1} K^{-1}); T, temperature (K). The parameters obtained were listed in Table 5.

The positive value of ΔH for the processes indicated that the adsorption of PS-APD for Au(III) was endothermic processes, which was consistent with the results of adsorption kinetics. The pos-

Table 4
Langmuir and Freundlich isotherm parameters and correlation coefficients for the adsorption PS-APD for Au(III) at different temperatures.

T (K)	Langmuir			Freundlich		
	Q_m (mmol g^{-1})	K_L (mL mmol^{-1})	R^2	K_F (mmol g^{-1})	n	R^2
298	1.414	18.01	0.9982	1.26	4.10	0.8648
308	1.437	25.89	0.9988	1.23	3.51	0.8166
318	1.443	40.31	0.9996	1.38	4.01	0.7260

itive value of ΔS results from the increased randomness due to the adsorption of Au(III) ion. The negative value of ΔG indicated that the feasibility of the process and the spontaneous nature of adsorption of Au(III) on the surface of PS-APD.

In order to determine whether the nature of adsorption processes is physical or chemical, the equilibrium data were also subjected to the *D–R* isotherm model. The linear form of the *D–R* isotherm equation [30] is:

$$\ln Q_e = \ln Q_m - \beta\varepsilon^2 \quad (16)$$

where β is the activity coefficient related to adsorption mean free energy ($mol^2\,J^{-2}$) and ε is the Polanyi potential ($\varepsilon = RT\ln(1 + 1/C_e)$).And the mean Gibb's free energy (E; $kJ\,mol^{-1}$) is calculated by using β value[31]:

$$E = \frac{1}{\sqrt{-2\beta}} \quad (17)$$

The *E* value gives information about adsorption mechanism, physical or chemical. If it lies between 8 and 16 $kJ\,mol^{-1}$, the adsorption process takes place chemically, while an *E* value of <8 $kJ\,mol^{-1}$ indicates the adsorption process proceeds physically [32,33]. The adsorption energy was calculated as 14.396 $kJ\,mol^{-1}$ (298 K) for the adsorption of Au(III) ion, suggesting that the adsorption processes of Au(III) ions onto PS-APD may be carried out by chemical adsorption.

3.7. Adsorption mechanism

The SEM images of PS-APD before and after adsorption were shown in Fig. 7. Obviously, there were a number of grains of elemental gold distributed on the surface of the resin after adsorption. It was probably because that redox reaction occurred after adsorption and Au(III) ion were reduced to Au(0).

Fig. 8 showed the IR spectra of PS-APD and PS-APD-Au. By comparison with that of PS-APD, the characteristic peaks of –COO– at 1697 cm^{-1} appeared in the curve of PS-APD-Au, and the characteristic absorption of C–O in PS-APD between 1030 and 1100 cm^{-1} was observed to decrease after the absorption, confirming that the PS-APD resin was oxidized.

The XPS of PS-APD before and after adsorption for Au(III) were showed in Fig. 9 and the binding energy data were listed in Table 6. A new 402.40 eV peak of N_{1s} binding energy appeared in PS-APD-Au in contrast to PS-APD and the binding energy value increased 2 eV, which demonstrated that electron donor nitrogen atom of PS-APD coordinated with Au(III) ion. The Au_{4f} binding energy of $AuCl_4^-$ adsorbed by PS-APD decreased obviously (2.55 eV) in contrast to $HAuCl_4$ and was similar to that of Au(0) in polyvinyl alcohol (PVA) matrix [34]. This meant that $AuCl_4^-$ was an electron acceptor and Au(III) ion might be reduced to Au(0) after adsorption. A similar phenomenon also has been found in the adsorption of polystyrene-supported glucosamine for Au(III) [35]. The adsorption mechanism may be expressed as Scheme 2, that is, Au(III) is easy to be reduced by alcohol hydroxyl group C–OH to form Au(0). In addition, the high loading capacity of PS-APD for Au(III) is possibly due to the release of adsorbed Au (III) from the resin body in Au(0) form and use of vacant sites by Au(III) in the solution phase that makes an adsorption [of Au(III)]–reduction [to Au(0)]–release [of Au(0)]–adsorption cycle [36].

Table 6
The binding energy (eV) of the adsorption of PS-APD for Au (III).

	C_{1s}	O_{1s}	N_{1s}	Au_{4f}
PS-APD	282.68 284.83 286.50	532.39	400.39	
PS-APD-Au	282.47 284.80 286.81	532.28	402.40	84.78
$HAuCl_4$				87.33
Au^0 (in PVA)				84.31

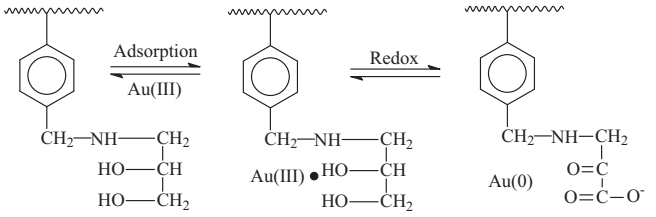

Scheme 2. The adsorption mechanism of PS-APD for Au (III).

3.8. Adsorption selectivity

A series of representative binary metal ion systems were chosen to investigate the adsorption selectivity of PS-APD for Au(III) and the results were shown in Table 7. Obviously, Au(III) was readily adsorbed by PS-APD from the systems of Au(III)–Pb(II), Au(III)–Cu(II), Au(III)–Ni(II), and Au(III)–Cu(II)–Pb(II), respectively, and adsorption percentage of PS-APD for Au(III) are more than 95%, indicating that PS-APD exhibited good adsorption selectivity for Au(III). This high adsorption selectivity was due to high affinity of the Au(III) ion for the amine group in PS-APD. According to the hard–soft acid–base (HSAB) theory, Au(III) is classified as a soft ion. Soft ions form very strong bonds with groups containing nitrogen and sulfur atoms [37].

Table 7 also lists Au(III) adsorption and separation on a number of adsorbents reported in the literature [38–41]. Compared to other

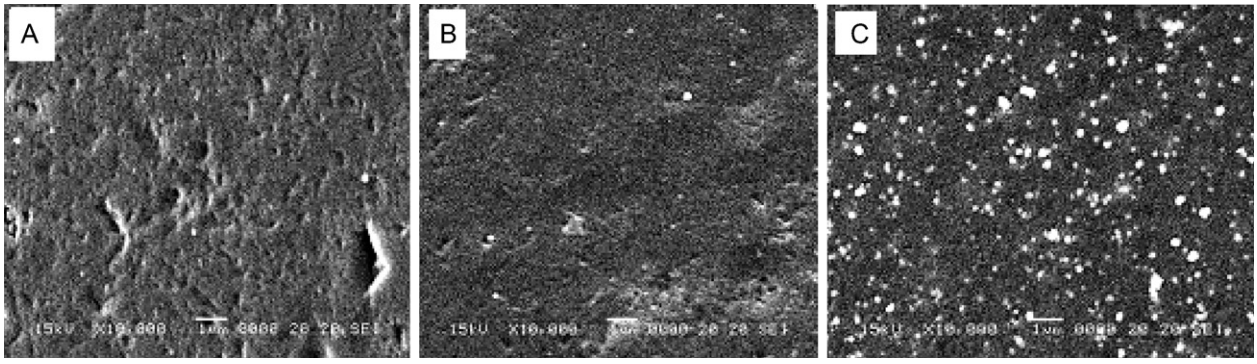

Fig. 7. The SEM images of A: PS-Cl, B: PS-APD and C: PS-APD-Au.

Fig. 8. Infrared spectar of PS-APD and PS-APD-Au.

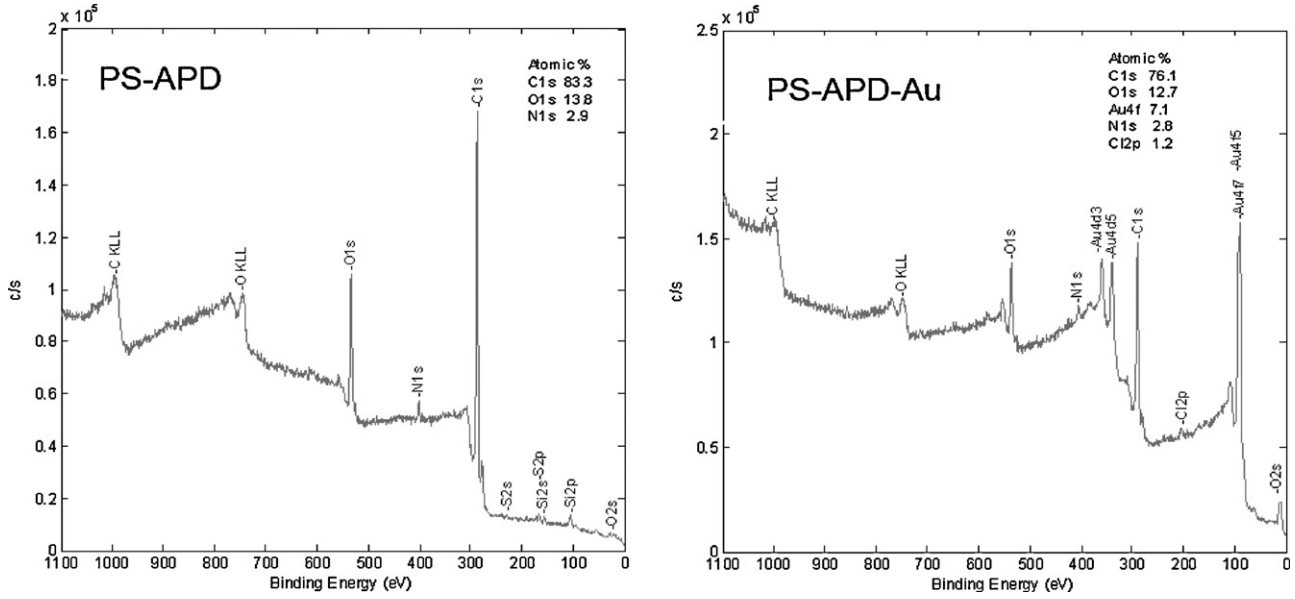

Fig. 9. X-ray photoelectron spectra of PS-APD and PS-APD-Au.

Table 7
The adsorption selectivity for Au(III) from multi-component systems.

Adsorbent	Composition	Selectivity[a]	Reference
PS-APD	Au(Ш),Hg(П)	2.49	This work
	Au(Ш), Pb(П)	3.57	
	Au(Ш),Cu(П)	3.72	
	Au(Ш),Ni(П)	3.53	
	Au(Ш),Cu(П),Pb(П)	3.26	
Duolite GT-73	Au(Ш),Cu(П), Ni(П),Pd(II)	1.90	[38]
Notren resin	Au(Ш),Cu(П)	1.27	[39]
Thiourea-formaldehyde resin	Au(Ш),Cu(П), Zn(П)	1.40	[40]
Urea-formaldehyde resin	Au(Ш),Cu(П), Zn(П)	1.62	
Chitosan	Au(Ш),Cu(П)	1.10	[41]
	Au(Ш),Cu(П), Ni(П), Co(II), Zn(П)	3.10	
	Au(Ш),Cu(П), Ni(П),Pd(II), Co(II), Zn(П)	0.33	
Silk sericin	Au(Ш),Cu(П)	2.60	
	Au(Ш),Cu(П), Ni(П), Co(II), Zn(П)	1.24	
	Au(Ш),Cu(П), Ni(П),Pd(II), Co(II), Zn(П)	2.76	

[a] Selectivity calculated according to Eq. (3).

adsorbents, PS-APD exhibits higher selectivity for Au(III), implying that PS-APD could probably be used in the extraction separation and recovery of Au(III) from a multi-ionic aqueous system.

4. Conclusions

A novel chelating resin PS-APD was prepared simply by the reaction of chloromethylated polystyrene with 3-amino-1,2-propanediol in this paper. IR spectra showed that APD group was successfully introduced into polystyrene matrix. The adsorption of PS-APD for Pb(II), Hg(II), Cu(II), Ni(II) and Au(III) ions were investigated. It was found that PS-APD resin possessed best enriching property to Au(III) ions among the metal ions and adsorption percentage could reach to about 99%. The adsorption dynamics of Au(III) showed that the pseudo second-order model was more suitable to describe the adsorption kinetics process. The investigation of adsorption isotherm showed that Langmuir model could describe the adsorption isothermal process of Au(III), and ΔG, ΔH, and ΔS values were calculated. The adsorption processes may be carried out by chemical adsorption because the sorption energy was calculated as 14.396 kJ mol^{-1} at 298 K. The adsorption mechanism of PS-APD for Au(III) was studied by means of SEM, IR, and XPS. The results showed that Au(III) ions might be reduced to Au(0) and the PS-APD resin were oxidized. Adsorption percentage of PS-APD for Au(III) in a series of representative binary metal ion systems are more than 0.95, indicating that PS-APD exhibited good adsorption selectivity for Au(III).

Acknowledgements

The authors are grateful for the financial support by the National Natural Science Foundation of China (grant no. 51073075), Natural Science Foundation of Shandong Province (nos. 2009ZRB01463, 2008BS04011), the Nature Science Foundation of Ludong University (nos. 08-CXA001, 032912, 042920) and Educational Project for Postgraduate of Ludong University (nos. YD05001, Ycx0612).

References

[1] J.M. Sanchez, M. Hidalgo, V. Salvado, The selective adsorption of gold (III) and palladium (II) on new phosphine sulphide-type chelating polymers bearing different spacer arms equilibrium and kinetic characterization, React. Funct. Polym. 46 (2001) 283–291.
[2] L. Peng, L. Guang, C. Da, C. Shao, T. Ning, Adsorption properties of Ag(I), Au(III), Pd(II) and Pt(IV) ions on commercial 717 anion-exchange resin, Trans. Nonferrous Met. Soc. China 19 (2009) 1509–1513.
[3] Y.Z. Zhao, The enrichment and separation of race gold, Pt and Pd from the ores based on co-precipitation, Gold 27 (2006) 42–44.
[4] C.P. Gomes, M.F. Almeida, J.M. Loureiro, Gold recovery with ion exchange used resins, Sep. Purif. Technol. 24 (2001) 35–57.
[5] R. Al-Merey, Z. Hariri, J. Abu Hilal, Selective separation of gold from iron ore samples using ion exchange resin, Microchem. J. 75 (2003) 169–177.
[6] S. Akita, L. Yang, H. Takeuchi, Solvent extraction of gold(III) from hydrochloric acid media by nonionic surfactants, Hydrometallurgy 43 (1996) 37–46.
[7] K.F. Lam, C.M. Fong, K.L. Yeung, Separation of precious metals using selective mesoporous adsorbents, Gold Bull. 40 (2007) 192–198.
[8] Y.C. Chang, D.H. Chen, Recovery of gold(III) ions by a chitosan-coated magnetic nano-adsorbent, Gold Bull. 39 (2006) 98–102.
[9] R.J. Qu, C.M. Sun, M.H. Wang, C.N. Ji, Q. Xu, Y. Zhang, C.H. Wang, H. Chen, P. Yin, Adsorption of Au(III) from aqueous solution using cotton fiber/chitosan composite adsorbents, Hydrometallurgy 100 (2009) 65–71.
[10] A. Ehrhardt, K. Miyazaki, Y. Sato c, T. Hori, Modified polypropylene fabrics and their metal ion sorption role in aqueous solution, Appl. Surf. Sci. 252 (2005) 1070–1075.
[11] M. Ghaedi, A. Shokrollahi, A.H. Kianfar, A. Pourfarokhi, N. Khanjari, A.S. irsadeghi, M. Soylak, Preconcentration and separation of trace amount of heavy metal ions on bis(2-hydroxy acetophenone)ethylendiimine loaded on activated carbon, J. Hazard. Mater. 162 (2009) 1408–1414.
[12] M. Yu, D. Sun, W. Tian, G. Wang, W. Shen, N. Xu, Systematic studies on adsorption of trace elements Pt, Pd, Au, Se, Te, As, Hg, Sb on thiol cotton fiber, Anal. Chim. Acta 456 (2002) 147–155.
[13] M.A. Congost, D. Salvatierra, G. Marquks, J.L. Bourdelande, J. Font, M. Valieinte, A novel phosphine sulphide functionalized polymer for the selective separation of Pd(I1) and Au(II1) from base metals, React. Funct. Polym. 28 (1996) 191–200.
[14] K. Dev, G.N. Rao, Preparation and analytical properties of a chelating resin containing bicine groups, Talanta 42 (1995) 591–596.
[15] B. Rivas, P. Ovando, S. Villegas, High-retention properties for Hg(II) ions of a resin containing ammonium and pyridine groups, J. Appl. Polym. Sci. 83 (2002) 2595–2599.
[16] L.Y. Jia, X.Q. Chen, J.T. Wei, Y. Liu, Synthesis of graft-P-tert-butylphenol resin and its adsorption capability of rubidium, J. Cent. South Univ. Technol. 32 (2001) 54–57.
[17] J. Huang, K. Huang, S. Liu, Q. Luo, S. Shi, Synthesis, characterization, and adsorption behavior of aniline modified polystyrene resin for phenol in hexane and in aqueous solution, J. Colloid Interface Sci. 317 (2008) 434–441.
[18] C.M. Sun, R.J. Qu, C.N. Ji, C.H. Wang, Y.Z. Sun, Z.W. Yue, G.X. Cheng, Preparation and adsorption properties of crosslinked polystyrene-supported low-generation diethanolamine-typed dendrimer for metal ions, Talanta 70 (2006) 14–19.
[19] P.M. Price, J.H. Clark, D.J. Macquarrie, Modified silicas for clean technology, J. Chem. Soc. Dalton Trans. (2000) 101–110.
[20] M. Tuzen, A. Sari, D. Mendil, M. Soylak, Biosorptive removal of mercury(II) from aqueous solution using lichen (Xanthoparmelia conspersa) biomass: kinetic and equilibrium studies, J. Hazard. Mater. 169 (2009) 263–270.
[21] S.P. Ramnani, S. Sabharwal, Adsorption behavior of Cr(VI) onto radiation crosslinked chitosan and its possible application for the treatment of wastewater containing Cr(VI), React. Funct. Polym. 66 (2006) 902–909.
[22] G. Rojas, J. Silva, J.A. Flores, A. Rodriguez, M. Ly, H. Maldonado, Adsorption of chromium onto cross-linked chitosan, Sep. Purif. Technol. 44 (2005) 31–36.
[23] Y.S. Ho, Citation review of Lagergren kinetic rate equation on adsorption reactions, Scientometrics 59 (2004) 171–177.
[24] Y.S. Ho, G. McKay, Pseudo-second order model for sorption processes, Process Biochem. 34 (1999) 451–465.
[25] W.J. Weber, J.C. Morris, Advances in water pollution research: removal of biologically resistant pollutants from waste waters by adsorption, in: Proceedings of the International Conference on Water Pollution Symposium, vol. 2, 1962, pp. 231–266.
[26] S.S. Gupta, K.G. Bhattacharyya, Adsorption of Ni(II) on clays, J. Colloid Interface Sci. 295 (2006) 21–32.
[27] Y.S. Ho, Selection of optimum sorption isotherm, Carbon 42 (2004) 2115–2116.
[28] H. Kitagawa, R. Suzuki, Foundation and Design of Adsorptions, (Z.L. Lu, Trans.), Chemical Industry Press, China, 1983.
[29] A.M. Donia, A.A. Atia, H.A. El-Boraey, D.H. Mabrouk, Adsorption of Ag(I) on glycidyl methacrylate/N,N′-methylene bis-acrylamide chelating resins with embedded iron oxide, Sep. Purif. Technol. 48 (2006) 281–287.
[30] M.M. Dubinin, E.D. Zaverina, L.V. Radushkevich, Sorption and structure of active carbons I. Adsorption of organic vapors, Zh. Fiz. Khim. 21 (1947) 1351–1362.
[31] F. Helfferich, Ion Exchange, McGraw Hill, NY, USA, 1962.
[32] I. Kiran, T. Akar, A.S. Ozcan, A. Ozcan, S. Tunali, Biosorption kinetics and isotherm studies of Acid Red 57 by dried cephalosporium aphidicola cells from aqueous solutions, Biochem. Eng. J. 31 (2006) 197–203.
[33] M.F. Sawalha, J.R.P. Videa, J.R. González, J.L. Gardea-Torresdey, Biosorption of Cd(II), Cr(III), and Cr(VI) by saltbush (*Atriplex canescens*) biomass: thermodynamic and isotherm studies, J. Colloid Interface Sci. 300 (2006) 100–104.
[34] C.M. Sun, R.J. Qu, C.N. Ji, Y.F. Meng, C.H. Wang, Y.Z. Sun, L.Y. Qi, Preparation and property of polyvinyl alcohol-based film embedded with gold nanoparticles, J. Nanopart. Res. 11 (2009) 1005–1010.
[35] C.M. Sun, R.J. Qu, Q. Wang, C.N. Ji, C.H. Wang, Q. Xu, X. Fang, G. Cheng, Synthesis and characterization of polystyrene-supported glucosamine resin and its adsorption behavior for Au(III), J. Appl. Polym. Sci. 100 (2006) 4581–4586.
[36] D. Parajuli, H. Kawakita, K. Inoue, K. Ohto, K. Kajiyama, Persimmon peel gel for the selective recovery of gold, Hydrometallurgy 87 (2007) 133–139.
[37] K.F. Lama, C.M. Fong, K.L. Yeung, G. Mckay, Selective adsorption of gold from complex mixtures using mesoporous adsorbents, Chem. Eng. J. 145 (2008) 185–195.
[38] M. Iglesias, E. Antico, V. Salvado, Recovery of palladium(II) and gold(III) from diluted liquors using the resin duolite GT-73, Anal. Chim. Acta 381 (1999) 61–67.
[39] G.W. Dicinoksi, Novel resins for the selective extraction of gold from copper rich ores, S. Afr. J. Chem. 53 (2000) 33–43.
[40] E. Ertan, M. Gulfen, Separation of gold(III) ions from copper(II) and zinc(II) ions using thiourea-formaldehyde or urea-formaldehyde chelating resins, J. Appl. Polym. Sci. 111 (2009) 2798–2805.
[41] X. Chen, K.F. Lam, S.F. Mak, K.L. Yeung, Precious metal recovery by selective adsorption using biosorbents, J. Hazard. Mater. 186 (2011) 902–910.